High-fidelity imaging using compact multi-frame blind deconvolution

Stuart M. Jefferies
Georgia State University, Atlanta, GA
Douglas Hope
Hope Scientific Renaissance LLC, Colorado Springs, CO
Cody Smith
Georgia State University, Atlanta, GA

ABSTRACT

Multi-frame blind deconvolution (MFBD) has been a cornerstone for ground-based space situational awareness of near-Earth satellites, since the early 2000's. In 2011, a variation of the classic MFBD algorithm was introduced that required solving for fewer variables than in the classic algorithm, but which still used all the available data to constrain the solution. The initial application of the new approach, referred to as compact multi-frame blind deconvolution (CMFBD), was found to be significantly faster than MFBD, and showed an indication that it may be able to provide restorations of higher quality (fewer artifacts).
Since its introduction, the CMFBD approach has become the foundation of several next-generation MFBD-based algorithms that have been developed for applications such as high-accuracy wave front sensing from image plane data, and imaging through strong turbulence: both of which contribute to space situational awareness by increasing the area of sky available for surveillance.
Here we show that the performance of the CMFBD approach can be improved through the addition of a new "internal consistency" constraint on the estimated point-spread functions.

1. BACKGROUND

Multi-frame blind deconvolution (MFBD) is an image restoration technique developed in the early 1990s [1,2] that allows for the reconstruction of an image from multiple blurred and noisy observations, without prior knowledge on the point-spread functions (PSFs) for the observations. With this capability, it is clear why MFBD has rapidly found application in numerous areas of research including astronomy, remote sensing, medical imaging, microscopy, and space situational awareness.

MFBD algorithms typically estimate the object and PSFs that describe the observed data through minimization of a cost function that has the form

$$\text{cost} = \text{data fit terms} + \text{prior terms}.$$

Here the data fit term compares the observed data with the model for the data generated from the object and PSF models. The 'prior terms' inject additional information that may be known about the imaging system or the noise processes corrupting the data. The underlying assumption is that the more prior information injected into the problem, the higher the fidelity of the solution. In principle, the quality of an MFBD restoration should improve as the number of frames increases. However, as the number of frames increases so too does the number of variables required to model all the data, and their estimation becomes impractical due the large dimensionality of the parameter hyperspace. This leads to inevitable entrapment in local minima during the optimization. That is, the weak link in non-linear blind image restoration is the optimization routine.

However, when using large data sets we can easily reduce the number of variables to be estimated by using a subset of the available image data. This subset of data, which are selected to provide high-signal-to-noise signal across a large fraction of the object's Fourier spectrum, can then be used for the estimation of the target object and the associated PSFs. This is, of course, just MFBD with frame selection. To use all of the data set to constrain our solution, we turn to compact MFBD (or CMFBD) [3]. In CMFBD we use the non-selected data frames to provide an additional constraint on the PSF estimates for the selected data frames. We refer to the former as non-control frames and the latter as control frames.

The constraint brought by the non-control frames is that the PSFs generated for these frames, using the estimated optical transfer functions (OTFs) for the control frames and the observed spectral ratios, are positive.
That is, the normal "(data – model)^2" least squares cost function for the control frames is supplemented with a positivity metric for the PSFs for the non-control frames,

$$\varepsilon_{pos} = \Sigma_k \Sigma_{j\neq k} \Sigma_x M_j(x)\, h_j(\mathbf{x})^2 \; ; \; M_j(x) = 1 \text{ if } h_j(\mathbf{x}) < 0, = 0 \text{ otherwise}, \tag{1}$$

where

$$h_j(\mathbf{x}) = |FT^{-1}\{H_k(\mathbf{u})\, \beta_{j,k}(\mathbf{u})\}_{\mathbf{x}}|^2, \tag{2}$$

$$\beta_{j,k}(\mathbf{u}) = [G_j^{obs}(\mathbf{u})/G_k^{obs}(\mathbf{u})], \tag{3}$$

the index k is over the frame-selected images, and the index j is over the remaining images (the non-control frames). The data frame, object and PSF estimates and their Fourier transforms are given by
$[g(\mathbf{x}), G(\mathbf{u})]$, $[f(\mathbf{x}),F(\mathbf{u})]$ and $[h(\mathbf{x}), H(\mathbf{u})]$, respectively.

The performance of the CMFBD algorithm was validated using data of the SEASAT satellite that were acquired during the daytime using a 1.6 m telescope. It was shown that the restoration from a CMFBD restoration was of higher fidelity and showed fewer artifacts than a restoration using a standard MFBD algorithm [4]. What is interesting here is that CMFBD does not capitalize on the information on the object that is available in the non-control frames. However, this is straightforward to overcome. Once the object and PSFs for the control frames have been estimated, we can use the recovered object in a forward deconvolution problem (i.e., hold $F(\mathbf{u})$ fixed) to provide good initial PSF estimates for the non-control frames. That is, we find the PSF estimate that minimizes the "(data – model)^2" cost function

$$\varepsilon_{conv} = \Sigma_j \Sigma_{\mathbf{u}} |G_j^{obs}(\mathbf{u}) - F(\mathbf{u})\hat{H}_j(\mathbf{u})|^2 \tag{4}$$

Once the PSFs for the non-control frames have been estimated, then the entire data set can be reduced to a single MFBD problem. The advantage of employing CMFBD as a first step in the blind image restoration process is that we are using high-quality initial estimates for the object and the PSFs, and the optimization algorithm now has a better chance of not getting trapped in a local minimum far from the global minimum.

This is now our standard approach and we have successfully used the CMFBD approach as a first step in all of our MFBD-based algorithms. This includes our aperture diversity and multi-aperture phase retrieval algorithms that perform well with imagery obtained through strong atmospheric turbulence, both in terms of image restoration and wave front sensing, respectively [5].

2. PSF CONSISTENCY METRIC

Here we argue that the non-control PSFs, via their optical transfer functions (OTFs) $\{H_j(\mathbf{u})\}$, estimated using the OTFs of all the different control frames, $\{H_k(\mathbf{u})\}$, should be the same, which gives us the constraint

$$\varepsilon\hat{} = \Sigma_u \Sigma_k \Sigma_{k'\neq k} M_{k,k'}(\mathbf{u})\, \Sigma_j M^H{}_j(\mathbf{u}) |\beta_{j,k}(\mathbf{u})H_k(u) - \beta_{j,k'}(\mathbf{u})H_{k'}(u)|^2 \tag{5}$$

where $M_{k,k'}(\mathbf{u})$ is a binary mask that is zero at spatial frequencies where the Fourier spectra $F(\mathbf{u})$, $H_k(\mathbf{u})$, and $H_{k'}(\mathbf{u})$ have spectral holes, and is unity elsewhere. Similarly, $M^H{}_j(\mathbf{u})$ is a binary mask that is zero at spatial frequencies where the Fourier spectrum H_j is zero, and is unity elsewhere.

The same argument also leads to an additional constraint for use during the estimation of the PSFs, for the non-control frames, after the CMFBD processing of the control frames, i.e.,

$$\varepsilon_j = \Sigma_{\mathbf{u}} M_{k,j}(\mathbf{u}) \,|\, A_j(\mathbf{u}) \exp(i\phi(\mathbf{u})) \bigstar A_j(\mathbf{u}) \exp(i\phi(\mathbf{u})) - \Sigma_{\mathbf{k}} H_k(\mathbf{u})\, \beta_{j,k}(\mathbf{u}) / K|^2 \tag{6}$$

where $A_j(\mathbf{u})$ and $\phi(\mathbf{u})$ are the amplitude and phase of the pupil function for the j^{th} frame, ★ denotes correlation, and *K* is the total number of control frames. We note that we estimate the PSFs via the inverse Fourier transform of the

autocorrelation of their wave fronts in the pupil. This ensures that the PSFs are positive, band-limited functions. The pupil amplitudes are assumed to be constant and uniform across the pupil.

3. RESULTS

We evaluate the performance of our updated CMFBD algorithm using the same ground-based imagery of SEASAT used in the validation of the original CMFBD algorithm.

For CMFBD processing of the image data we minimize the cost function

$$\varepsilon = \varepsilon_c + \alpha\varepsilon_{pos} + \gamma\varepsilon\hat{} \tag{8}$$

where

$$\varepsilon_c = \Sigma_{\mathbf{u}} \Sigma_k |g_k(x) - g_k^{obs}(x)|^2, \tag{9}$$

and α and γ are weighting functions (set to 0.1). The variables in the minimization are the square root of the pixel values of the object estimate, and the pupil plane pixels for the PSF estimates as described in [3]. We selected a sub-set of 36 frames from the 271-frame data set as our control frames using the frame selection algorithm described in [3]. For the conventional MFBD processing of the data, we used the algorithm of [6].

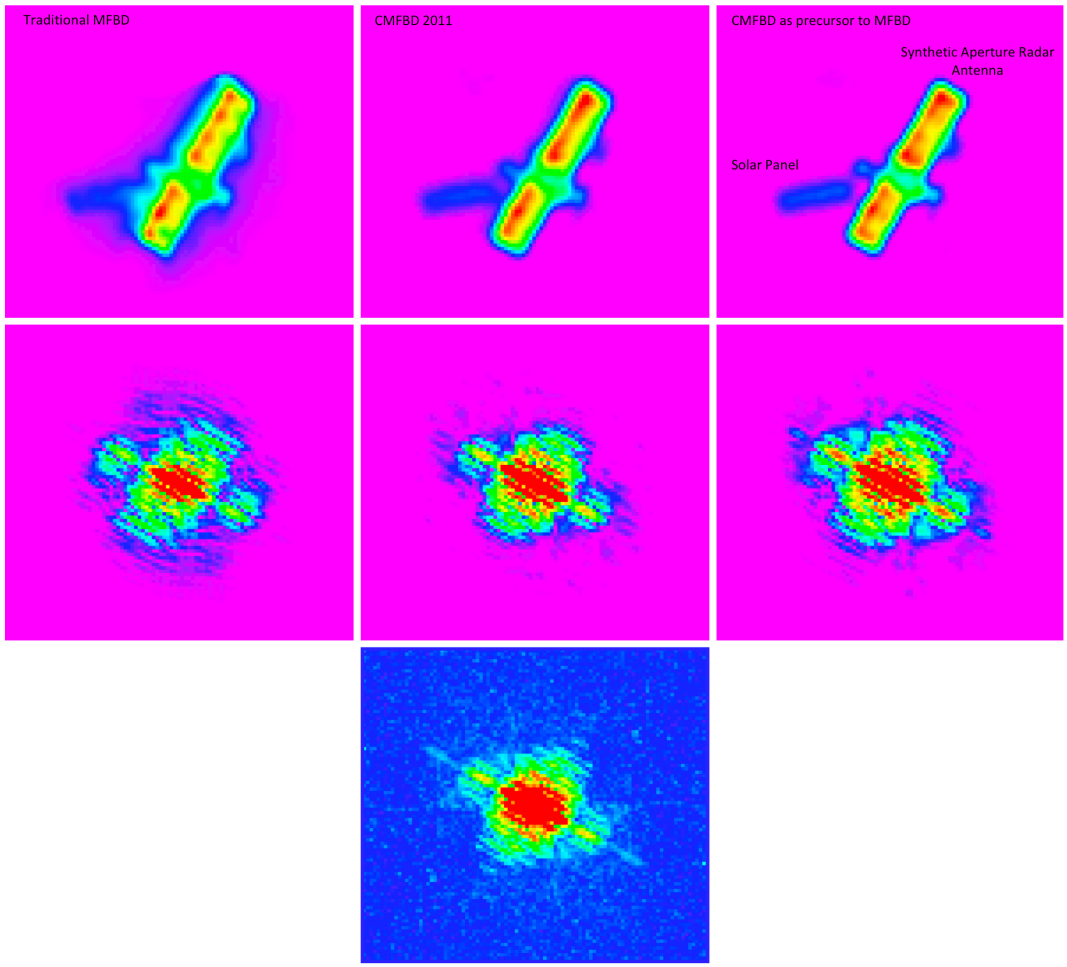

Fig. 1. Top Row (left to right): MFBD restoration (271 frames), CMFBD restoration (36 frames), MFBD restoration with CMFBD initial step (271 frames). Middle row (left to right): Fourier amplitude spectra for the objects in the top row and corresponding column. Bottom row (center): Spectrum showing maximum Fourier amplitude in the data set at each spatial frequency. This shows the morphology of the Fourier spectrum for the object.

The results are shown in Fig. 1. The improvement in quality of the CMFBD restoration over the restoration of the full 271-frame data set using conventional MFBD is clearly demonstrated. There are significantly fewer artifacts and the edges of structures on the satellite are crisper, in particular, the synthetic aperture radar antenna in the foreground and the solar panels in the background. The presence of a high level of artifacts in the MFBD image can also be seen when we compare the Fourier amplitude spectrum of the restored image, with the spectrum that shows the maximum Fourier amplitude at each spatial frequency for the whole data set: the morphology of the spectrum of the CMFBD restoration is very similar to that of the spectrum derived from the entire data set, whereas the spectrum of the MBFD restoration is quite different.

In a second step, we use the CMFBD estimates for the object and the PSFs for the control frames, along with the estimates of the PSFs for the non-control frames obtained using eqn. 6, in a 271-frame MFBD restoration. This way we use the entire data set to provide information on the target satellite. The spectrum of the restored object from the second step (right column of Fig. 1) shows that the restoration has essentially diffraction-limited resolution. The improvement in image quality can be seen by the increased sharpness in the solar panels at the rear of the satellite, and the more uniform intensity distribution across the synthetic aperture radar antenna at the front of the satellite. We note that the low level artifacts in the background away from the satellite are the result of poor image calibration of the raw data, and should vanish with improved calibration.

4. CONCLUSIONS

We have shown that the performance of the CMFBD approach can be improved through the addition of a new "internal consistency" constraint on the estimated point-spread functions. When using CMFBD as a first step in a MFBD restoration of an entire data set, the enhanced performance of CMFBD leads to an improvement in the performance of the MFBD restoration. In our proof-of-concept example, we were able to produce a restored image that exhibited diffraction limited resolution, from atmospheric turbulence-degraded imagery obtained with a 1.6m aperture telescope, without the use of adaptive optics. We expect to see analogous improvements in performance for our other algorithms that use CMFBD as a first step (e.g., [5]).

5. ACKNOWLEDGEMENTS

This work was supported by award FA9550-14-1-0178 from the Air Force Office of Scientific Research.

6. REFERENCES

1 Schulz, T. J., Multi-frame blind deconvolution of astronomical images, JOSA A., 10, 1064-1073, 1993.
2 Jefferies, S. M. and Christou, J., Restoration of Astronomical Images by Iterative Blind Deconvolution, ApJ, 415, 862-864, 1993.
3 Hope, D. A. and Jefferies, S. M., Compact multi-frame blind deconvolution, Optics Letters, 36, 867-869, 2011.
4 Hope, D. A and Jefferies, S. M., Multi-frame blind deconvolution: compact and multi-channel versions, *Proceedings of the Advanced Maui Optical and Space Surveillance Technologies Conference*, held in Wailea, Maui, September 2011, Ed: S. Ryan, The Maui Economic Development Board, p. E39, 2011.
5 Hope, D., Jefferies, S. M., Hart, M. and Nagy, J., High-resolution speckle imaging through strong atmospheric turbulence, Optics Express, 24, 12116-12129, 2016.
6 Matson, C. L., Borelli, K., Jefferies, S. M., Hege, Beckner, C. C., E. K. and Lloyd-Hart, M., "A Fast and Optimal Multi-Frame Blind Deconvolution Algorithm for High-Resolution, Ground-Based Imaging of Space Objects", Applied Optics, 48, A75-A92, 2009.